

# Hybrid-Driven-Based $\mathcal{H}_\infty$ Control for Networked Cascade Control Systems With Actuator Saturations and Stochastic Cyber Attacks

Jinliang Liu<sup>1</sup>, Yuanyuan Gu<sup>1</sup>, Xiangpeng Xie<sup>1</sup>, Dong Yue<sup>1</sup>, and Ju H. Park<sup>2</sup>

**Abstract**—This paper focuses on the hybrid-driven-based  $\mathcal{H}_\infty$  control for networked cascade control systems (NCCSs) with actuator saturations and stochastic cyber attacks. In order to relieve the network bandwidth load effectively, a hybrid triggered scheme is introduced, which contains a switch between time-triggered scheme and event-triggered scheme. A newly hybrid-driven-based NCCS model is established by considering the effects of both actuator saturations and stochastic cyber attack, which is an important threat to network security. By using the Lyapunov stability theory, sufficient conditions are obtained to ensure the system stability. Furthermore, both primary controller gain and secondary controller gain are achieved explicitly in terms of linear matrix inequality techniques. Finally, a power plant gas-turbine system is presented to illustrate the usefulness of the designed state feedback controllers.

**Index Terms**—Actuator saturations, cyber attacks, hybrid triggered scheme, networked cascade control systems (NCCSs).

## I. INTRODUCTION

IN RECENT years, cascade control has exhibited widely industrial applications such as chemical reactors [1], power plants [2], underwater robots [3], networked control systems (NCSs) [4], and so on. Its success mainly depends on the distinctive structure composed of two control loops where the outer loop is responsible for the stability of the systems and the inner loop is aimed at eliminating the disturbances quickly [4]. NCS is a kind of control system where sensors, controllers and actuators are connected through a communication network [13], the advantages of which are simple installation, easy maintenance and low cost, etc. [5]. It is

worth noting that an increasing attention has been paid to the combination of cascade control and NCS in the past decade, which is called networked cascade control systems (NCCSs). For example, a typical kind of NCCS with state feedback controllers is investigated and the sufficient condition for the stability of NCCS as well as the  $\mathcal{H}_\infty$  control laws are obtained in [4]. A class of NCCSs based on fieldbus is studied in [6], which is modeled as a finite-dimensional discrete-time linear time-invariant system in terms of augmented state vector method. The stabilization and  $\mathcal{H}_\infty$  controller design problems are investigated in [7], which are based on an extended model called singular NCCSs. For singular NCCSs, the problem of dissipative fault-tolerant control synthesis and the issue of exponential passivity analysis are further addressed in [8] and [9], respectively.

However, the introduction of the network also brings about many challenges including network-induced time-delay [10], limited network bandwidth [11], and packet dropout [12], which may deteriorate the performance and destabilize the system. How to prevent the data from redundant signal transmissions has been a fundamental research topic in control and signal processing areas. From an analysis and design point of view [13], time-triggered scheme has been widely adopted for many years since it simply transmits all periodically sampled data to guarantee a desired system performance [14]. However, from a computation and resource occupation point of view [15], it will send unnecessary signals to the bandwidth-limited communication channel and give rise to the waste of network resources in such case that the system state keeps steady [19]. In order to decrease the overload of network bandwidth [16] resulting from the time-triggered scheme, many scholars have proposed various event-triggered schemes [17]. For example, a novel event-triggered scheme is proposed in [14], which can effectively reduce the burden of network bandwidth. The main idea of the event-triggered scheme proposed in [14] is that the newly sampled data whether to be transmitted or not is determined by a threshold. There has been a rich body of research results available in the literature based on the event-triggered scheme mentioned in [14]. For example,  $\mathcal{H}_\infty$  filtering problem for sampled-data systems is studied in [18] by adopting the event-triggered scheme in [14] to save communication resources. Peng *et al.* [19] proposed a novel mixed self-triggered and event-triggered scheme to improve the energy efficiency of the wireless sensor networks, which extends the event-triggered scheme proposed in [14].

Manuscript received July 3, 2018; accepted October 2, 2018. Date of publication October 30, 2018; date of current version November 19, 2019. This work was supported in part by the National Natural Science Foundation of China under Grant 61403185 and Grant 61473156, and in part by the Natural Science Foundation of Jiangsu Province of China under Grant BK20171481. The work of J. H. Park was supported by the Basic Science Research Programs through the National Research Foundation of Korea (NRF) funded by the Ministry of Education under Grant NRF-2017R1A2B2004671. This paper was recommended by Associate Editor M. Basin. (Corresponding author: Ju H. Park.)

J. Liu and Y. Gu are with the College of Information Engineering, Nanjing University of Finance and Economics, Nanjing 210023, China (e-mail: liujinliang@vip.163.com; guyuanyuan0203@163.com).

X. Xie and D. Yue are with the Institute of Advanced Technology, Nanjing University of Posts and Telecommunications, Nanjing 210023, China (e-mail: xixiangpeng1953@163.com; medongyue@vip.163.com).

J. H. Park is with the Department of Electrical Engineering, Yeungnam University, Kyonsan 38541, South Korea (e-mail: jessie@ynu.ac.kr).

Color versions of one or more of the figures in this paper are available online at <http://ieeexplore.ieee.org>.

Digital Object Identifier 10.1109/TSMC.2018.2875484

Inspired by the event-triggered scheme proposed in [14], the problem concerning decentralized event-triggered  $\mathcal{H}_\infty$  control is addressed in [20] for neural networks. By combining the advantages of both time-triggered scheme and event-triggered scheme proposed in [14], a novel hybrid triggered scheme is proposed in [21], which is implemented by a random switching between time-triggered scheme and event-triggered scheme, and the adoption of hybrid triggered scheme can improve the system performance and reduce the network transmission simultaneously. Under the hybrid triggered scheme proposed in [21], the quantized stabilization and the  $\mathcal{H}_\infty$  filter design problem for T-S fuzzy systems are investigated in [22] and [23], respectively. In addition, Liu *et al.* [24] designed the resilient observer-based output feedback controller for T-S fuzzy systems under the hybrid triggered scheme [21].  $\mathcal{H}_\infty$  filter design for networked systems [25] and for neural networks [26] are, respectively, addressed by considering the hybrid triggered scheme mentioned in [21].

As is well known, owing to the physical constraints or technological restrictions, saturation phenomena inevitably exist in different kinds of practical systems [31], which may also deteriorate the performance of the systems [32], [33]. Actuator saturation is one of the most important saturation phenomena [34], which has attracted lots of attention. For instance, an anti-windup controller is designed in [35] for singularly perturbed systems with actuator saturation. The issue of adaptive fuzzy tracking control is studied in [36] for nonlinear stochastic systems by considering actuator saturation. Wang *et al.* [37] proposed a global cooperative control framework to address the global leader-follower consensus for multiagent systems subject to actuator saturation. The event-triggered control for linear systems is presented in [38] with actuator saturation and external disturbances.

More recently, due to the open property of data transmission channels, the security problems in NCSs have gained an ever-increasing interest from researchers in the control community [39], [40]. In particular, cyber attacks have become the major threat to network security, which aim to affect the control performance by destroying/modifying certain significant data transmitted over network [41]. Hence, increasing research interests have been paid to exploring the impact coming from various cyber attacks such as denial of service attacks [42], replay attacks [43], and deception attacks [44]. For example, Ding *et al.* [45] investigated the observer-based event-triggering consensus control for a class of discrete-time multiagent systems by considering lossy sensors and cyber-attacks. Distributed event-triggered control problem is addressed in [46] for NCSs with stochastic cyber-attacks. Distributed recursive filter for stochastic systems and distributed event-triggered  $\mathcal{H}_\infty$  filter for continuous-time linear-invariant system are separately designed in [47] and [48] over sensor networks, where the deception attacks randomly take place.

Motivated by the previously mentioned results, this paper first investigates the problem of  $\mathcal{H}_\infty$  control for NCCSs with hybrid triggered scheme, actuator saturations and stochastic cyber attacks. The main contributions are summarized as follows.

- 1) The hybrid triggered scheme is first introduced into the  $\mathcal{H}_\infty$  controller design problem for NCCSs while taking

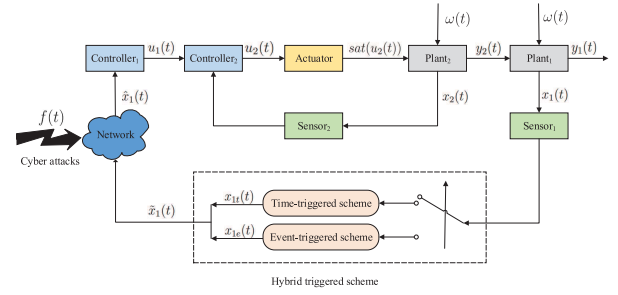


Fig. 1. Structure of hybrid-driven-based  $\mathcal{H}_\infty$  controller for NCCSs with actuator saturations and stochastic cyber attacks.

the effects of actuator saturations and stochastic cyber attacks into consideration.

- 2) A new model for NCCSs is first constructed by considering the hybrid triggered scheme, actuator saturations and stochastic cyber attacks.
- 3) Based on the constructed model, the criteria for the considered NCCSs stability are derived by means of Lyapunov stability theory. Moreover, the primary controller gain and the secondary controller gain are obtained simultaneously in terms of linear matrix inequality (LMI) techniques.

The remainder of this paper is organized as follows. In Section II, problem formulation and preliminaries are outlined and a new model for NCCSs is established. Section III shows the main results concerning the sufficient stabilization conditions for NCCSs and the  $\mathcal{H}_\infty$  controller design method. Moreover, both primary controller gain and secondary controller gain are obtained. An illustrative example is given in Section IV to show the usefulness of the design method. Conclusion is presented in Section V.

*Notation:*  $\mathbb{R}^n$  and  $\mathbb{R}^{n \times m}$  stand for the  $n$ -dimensional Euclidean space and the set of  $n \times m$  real matrices, respectively; the superscript T represents matrix transposition;  $I$  denotes the identity matrix of appropriate dimension; the notation  $X > 0$  for  $X \in \mathbb{R}^{n \times n}$  means that the matrix  $X$  is real symmetric positive definite;  $\mathbb{E}$  is the expectation operator;  $*$  refers to the entries caused by symmetry;  $\|\cdot\|$  denotes the Euclidean norm; and  $\text{sym}(B)$  represents the symmetrized expression  $B + B^T$ .

## II. SYSTEM DESCRIPTION

This paper is concerned with hybrid-driven-based  $\mathcal{H}_\infty$  control for NCCSs with actuator saturations and stochastic cyber attacks. As shown in Fig. 1, the structure of cascade control system contains two loops, where the inner loop is made up of secondary plant Plant<sub>2</sub>, secondary sensor Sensor<sub>2</sub>, secondary controller Controller<sub>2</sub>, and actuator, and the outer loop is made up of primary plant Plant<sub>1</sub>, primary sensor Sensor<sub>1</sub>, primary controller Controller<sub>1</sub>, and actuator. A network is assumed to connect the Sensor<sub>1</sub> and the Controller<sub>1</sub> in the cascade control system, which constitutes the NCCS considered in this paper.

The primary plant Plant<sub>1</sub> under consideration is described by the following:

$$\text{Plant}_1 : \begin{cases} \dot{x}_1(t) = A_1 x_1(t) + B_1 y_2(t) \\ y_1(t) = C_1 x_1(t) + D_1 \omega(t) \end{cases} \quad (1)$$

where  $x_1(t) \in \mathbb{R}^n$  and  $y_1(t) \in \mathbb{R}^m$  denote the state vector and the measurement output of Plant<sub>1</sub>, respectively;  $y_2(t)$  is the measurement output of Plant<sub>2</sub>;  $\omega(t) \in \mathcal{L}_2[0, \infty)$  is the disturbance input; and  $A_1, B_1, C_1$ , and  $D_1$  are the known real constant matrices with appropriate dimensions.

The aim of this paper is to design hybrid-driven-based  $\mathcal{H}_\infty$  controllers for NCCSs with actuator saturations and stochastic cyber attacks. It can be seen from Fig. 1 that  $u_1(t)$  is the output of primary controller, as well as a part of the input of secondary controller. The given primary controller and the secondary controller are state feedback as follows:

$$\begin{cases} u_1(t) = K_1 \hat{x}_1(t) \\ u_2(t) = u_1(t) + K_2 x_2(t) \end{cases} \quad (2)$$

where  $K_1$  and  $K_2$  are the state feedback gain matrices of Controller<sub>1</sub> and Controller<sub>2</sub>, respectively;  $\hat{x}_1(t)$  is the real input of primary controller;  $x_2(t)$  is the state vector of secondary plant; and  $u_2(t)$  is the output of secondary controller.

*Remark 1:* Compared with the structure of common NCSs, the NCCSs have one more loop, which is added to quickly eliminate the disturbances in the inner loop. The key idea of this paper is to design useful primary controller in the outer loop and the secondary controller in the inner loop for NCCSs simultaneously.

Inspired by the idea of [21], a hybrid triggered scheme is introduced to alleviate the load of network bandwidth. As shown in Fig. 1, the hybrid triggered scheme contains a random switch between the “time-triggered scheme” and the “event-triggered scheme.”

When the switch turns on the channel of time-triggered scheme, the periodically sampled measurements will be transmitted in time, which implies that the sequence of transmitting instant is  $t_k h$  ( $k = 1, 2, \dots$ ), where  $h$  is a sampling period,  $t_k$  ( $k = 1, 2, \dots$ ) is a sequence set of positive integers, namely,  $\{t_1, t_2, t_3, \dots\} = \{1, 2, 3, \dots\}$ . In other words, when the latest transmitting instant is  $t_k h$ , the next transmitting instant is  $t_{k+1} h = t_k h + h$ . Suppose  $\eta_{t_k}$  denotes the network-induced time-delay of sensor measurement sampled at the instant  $t_k h$ .

Define  $\eta(t) = t - t_k h$ , as shown in Fig. 1, the sensor measurement can be described as

$$\begin{aligned} x_{1t}(t) &= x_1(t_k h) = x_1(t - \eta(t)) \\ t &\in [t_k h + \eta_{t_k}, t_{k+1} h + \eta_{t_{k+1}}), \quad k = 1, 2, \dots \end{aligned} \quad (3)$$

where  $0 < \min\{\eta_{t_k}\} \leq \eta(t) \leq \eta_M$ .  $\eta_M = h + \max\{\eta_{t_k}, \eta_{t_{k+1}}\} \triangleq h + \bar{\eta}$  and  $\bar{\eta}$  is the upper bound of the communication time-delay.

When the switch turns on the channel of event-triggered scheme, the periodically sampled measurements will be transmitted only when they violate the triggering condition. Then the sequence of transmitting instant can be expressed as follows:

$$\begin{aligned} t_{k+1} h &= t_k h + \inf_{j \geq 1} \left\{ j h | e_k^T(t) \Omega e_k(t) \right. \\ &\quad \left. > \lambda x_1^T(i_k^j h) \Omega x_1(i_k^j h) \right\}, \quad j = 1, 2, \dots \end{aligned} \quad (4)$$

where  $e_k(t) = x_1(t_k h) - x_1(i_k^j h)$ , the trigger parameters  $\Omega > 0$  will be designed and  $\lambda \in [0, 1)$  will be given.  $t_k h$  and  $i_k^j h =$

$t_k h + j h$  stand for the latest transmitting instant and current sampling instant, respectively.

By considering the effect of network, the transmitted data arriving at primary controller will be hold by zero-order-hold within the time interval  $[t_k h + \eta_{t_k}, t_{k+1} h + \eta_{t_{k+1}})$ . For development, the interval can be divided into several subintervals, which can be expressed as  $[t_k h + \eta_{t_k}, t_{k+1} h + \eta_{t_{k+1}}) = \cup_{j=0}^{d_k} [i_k^j h + \eta_{t_{k+j}}, i_k^{j+1} h + \eta_{t_{k+j+1}})$ , where  $d_k = t_{k+1} - t_k - 1$  is similar to the definition in [14]. Define  $d(t) = t - i_k^j h$ ,  $t \in [i_k^j h + \eta_{t_{k+j}}, i_k^{j+1} h + \eta_{t_{k+j+1}})$ ,  $j = 0, 1, 2, \dots$ . It is easy to get the range of  $d(t)$  as  $0 < \eta_{t_k} \leq d(t) \leq h + \max\{\eta_{t_k}, \eta_{t_{k+1}}\} = h + \bar{\eta} \triangleq d_M$ .

Then, the sensor measurement can be expressed as

$$\begin{aligned} x_{1e}(t) &= x_1(t_k h) = x_1(t - d(t)) + e_k(t) \\ t &\in [t_k h + \eta_{t_k}, t_{k+1} h + \eta_{t_{k+1}}). \end{aligned} \quad (5)$$

In order to explain the random switching rule of hybrid triggered scheme, a Bernoulli random variable  $\alpha(t)$  is introduced, where  $\alpha(t) \in \{0, 1\}$  and the statistical properties of  $\alpha(t)$  are assumed to be  $\mathbb{E}\{\alpha(t)\} = \bar{\alpha}$  and  $\mathbb{E}\{(\alpha(t) - \bar{\alpha})^2\} = \sigma^2$ . Then, as the method proposed in [21], the sensor measurement under hybrid triggered scheme can be described as follows:

$$\tilde{x}_1(t) = \alpha(t) x_{1t}(t) + (1 - \alpha(t)) x_{1e}(t). \quad (6)$$

*Remark 2:* The Bernoulli random variable  $\alpha(t)$  shown in (6) is utilized to indicate the switching law from one triggered scheme to another. If  $\alpha(t) = 1$ , the channel of time-triggered scheme is activated for transmitting. If  $\alpha(t) = 0$ , the channel of event-triggered scheme is chosen to transmit data.

*Remark 3:* The hybrid triggered scheme is first proposed in [21] to improve the system performance and reduce the network transmission for NCSs. This paper introduces the hybrid triggered scheme into the analysis and design for NCCSs with actuator saturations and stochastic cyber attacks.

In this paper, it is assumed that the cyber attacks are launched randomly which can be expressed by a nonlinear function  $f(x_1(t))$  and the corresponding time delay is assumed as  $\tau(t) \in (0, \tau_M]$ . Inspired by the method in [41] and [47], a Bernoulli random variable  $\beta(t)$  is utilized to govern the stochastic cyber attacks similarly. Furthermore, suppose  $\beta(t)$  is subject to Bernoulli distribution and uncorrelated to  $\alpha(t)$ . When  $\beta(t) = 1$ , the cyber attacks are implemented; otherwise, when  $\beta(t) = 0$ , the data transmission is normal. Therefore, under hybrid triggered scheme and stochastic cyber attacks, the real input of primary controller can be represented as

$$\hat{x}_1(t) = \beta(t) f(x_1(t - \tau(t))) + (1 - \beta(t)) \tilde{x}_1(t) \quad (7)$$

where  $\mathbb{E}\{\beta(t)\} = \bar{\beta}$  and  $\mathbb{E}\{(\beta(t) - \bar{\beta})^2\} = \delta^2$ .

*Remark 4:* For the NCCSs considered in this paper, a network is adopted to transmit data from primary sensor Sensor<sub>1</sub> to primary controller Controller<sub>1</sub>. In the practical engineering, the data transmission network is susceptible to be attacked by potential cyber attack, which is one of the important factors affecting the network security. It is notable that the successfully cyber attacks possess stochastic characteristic due mainly to the protection of hardware or software, the communication protocols and the randomly fluctuated network conditions



(e.g., network load, network congestion, and network transmission rate) [47]. For example, under a  $(T, N)$  secret sharing scheme, where a confidential message is divided into  $N$  shares and at least  $T$  out of  $N$  shares can reconstruct the original message, a secure message can be recovered only when  $T$  or more shares are successfully delivered by multipath routing protocol. In other words, if the cyber attacks randomly destroy the  $N$  different paths such that  $T - 1$  or less shares eventually arrive at destination host, the secure message will not be recovered [44]. To be more exact, the cyber attacks discussed in this paper belong to stochastic deception attacks, where the way of corrupting the transmission data is to fully substitute it with the attack signals [41].

*Remark 5:* It should be mentioned that the cyber attacks may be undetectable since the attack signals are strategically generated by malicious adversaries and may relate to system information [40]. This paper assumes the adversaries have access to full state information of Plant<sub>1</sub> (1). Moreover, similar to the description in [26], this paper models the cyber attacks as a nonlinear function associated with system state, which is confined in Assumption 1.

*Remark 6:* Note that upon the deception attacks occurring at any time during the data transmission over a network, the real measurements are replaced by attack signals which will cheat existing monitoring systems [39] and continue to be transmitted over a network. Thus, the attack signals are also subject to time delays, which are assumed to be bounded by  $\tau_M$  in this paper.

Then, the controllers of (2) can be rewritten as follows:

$$\begin{cases} u_1(t) = \beta(t)K_1f(x_1(t - \tau(t))) \\ \quad + (1 - \beta(t))\alpha(t)K_1x_1(t - \eta(t)) \\ \quad + (1 - \beta(t))(1 - \alpha(t))K_1x_1(t - d(t)) \\ \quad + (1 - \beta(t))(1 - \alpha(t))K_1e_k(t) \\ u_2(t) = u_1(t) + K_2x_2(t). \end{cases} \quad (8)$$

The secondary plant under consideration is described by the following:

$$\text{Plant}_2 : \begin{cases} \dot{x}_2(t) = A_2x_2(t) + A_3x_2(t - \theta(t)) \\ \quad + B_2\text{sat}(u_2(t)) + B_3\omega(t) \\ y_2(t) = C_2x_2(t) + D_2\omega(t) \end{cases} \quad (9)$$

where  $\theta(t) \in (0, \theta_M]$  is a state-delay variable of the Plant<sub>2</sub>;  $A_2, A_3, B_2, B_3, C_2$ , and  $D_2$  are the known real constant matrices with appropriate dimensions; and  $\text{sat}(u_2(t))$  is the saturation function of actuator, which has the similar definition in [34] as  $\text{sat}(u_2) = [\text{sat}(u_2^1), \text{sat}(u_2^2), \dots, \text{sat}(u_2^m)]^T \in \mathbb{R}^m$ , where

$$\text{sat}(u_2^i) \triangleq \begin{cases} \rho_i, & u_2^i > \rho_i \\ u_2^i, & -\rho_i \leq u_2^i \leq \rho_i, \\ -\rho_i, & u_2^i < -\rho_i \end{cases} \quad i = 1, 2, \dots, m \quad (10)$$

with  $\rho_i$  representing the known upper limits of actuator saturation constraints.

Borrowed the main idea of [34], the saturation function  $\text{sat}(u_2(t))$  can be represented by a linear  $u_2(t)$  and a nonlinear  $\phi(u_2(t))$ , namely

$$\text{sat}(u_2(t)) = u_2(t) - \phi(u_2(t)). \quad (11)$$

The dead-zone nonlinearity function  $\phi(u_2(t))$  satisfies the condition: there  $\exists 0 < \varepsilon < 1$ , such that

$$\varepsilon u_2^T(t)u_2(t) \geq \phi^T(u_2(t))\phi(u_2(t)) \quad (12)$$

where  $\varepsilon = \max\{\varepsilon_1, \varepsilon_2, \dots, \varepsilon_m\}$ .

*Remark 7:* According to the proof in [34], the  $\varepsilon$  in (12) is dependent on the factors as  $\rho_i$  and  $u_2^i$  in (10), namely, for  $i = 1, 2, \dots, m$ ,  $\varepsilon_i \geq (1 - (\rho_i/|u_2^i|_{\max}))^2$ , where  $|u_2^i|_{\max}$  stands for the maximum amplitude of control input  $u_2^i(t)$ .

Substitute  $u_2(t)$  in (8) into (11) and then the actuator saturation function  $\text{sat}(u_2(t))$  can be rewritten as

$$\begin{aligned} \text{sat}(u_2(t)) &= (1 - \beta(t))\alpha(t)K_1x_1(t - \eta(t)) \\ &\quad + (1 - \beta(t))(1 - \alpha(t))K_1x_1(t - d(t)) \\ &\quad + (1 - \beta(t))(1 - \alpha(t))K_1e_k(t) \\ &\quad + \beta(t)K_1f(x_1(t - \tau(t))) \\ &\quad + K_2x_2(t) - \phi(u_2(t)). \end{aligned} \quad (13)$$

By combining (1), (9), and (13), it can yield a new model for NCCSs as follows:

$$\begin{cases} \dot{x}_1(t) = A_1x_1(t) + B_1C_2x_2(t) + B_1D_2\omega(t) \\ \dot{x}_2(t) = A_2x_2(t) + A_3x_2(t - \theta(t)) \\ \quad + (1 - \beta(t))\alpha(t)B_2K_1x_1(t - \eta(t)) \\ \quad + (1 - \beta(t))(1 - \alpha(t))B_2K_1x_1(t - d(t)) \\ \quad + (1 - \beta(t))(1 - \alpha(t))B_2K_1e_k(t) \\ \quad + \beta(t)B_2K_1f(x_1(t - \tau(t))) \\ \quad + B_2K_2x_2(t) - B_2\phi(u_2(t)) + B_3\omega(t) \\ y_1(t) = C_1x_1(t) + D_1\omega(t). \end{cases} \quad (14)$$

In the following, an assumption and two lemmas are introduced, which are helpful to derive our desired results.

*Assumption 1* [26]: Assume that the following condition of nonlinear function  $f(x)$  holds, which is introduced to restraint the cyber attacks

$$\|f(x)\|^2 \leq \|Fx\|^2 \quad (15)$$

where  $F$  is a constant matrix standing for the upper bound of the nonlinearity.

*Lemma 1* [27]: Consider a given matrix  $R = R^T > 0$ . Then, for all continuously differentiable function  $\dot{x}(t)$  in  $[a, b] \rightarrow \mathbb{R}^n$ , the following inequality holds:

$$-\int_a^b \dot{x}^T(s)R\dot{x}(s)ds \leq -\frac{1}{b-a} \begin{bmatrix} \Pi_1 \\ \Pi_2 \end{bmatrix}^T \begin{bmatrix} R & * \\ 0 & 3R \end{bmatrix} \begin{bmatrix} \Pi_1 \\ \Pi_2 \end{bmatrix} \quad (16)$$

where

$$\begin{aligned} \Pi_1 &= x(b) - x(a) \\ \Pi_2 &= x(b) + x(a) - \frac{2}{b-a} \int_a^b x(s)ds. \end{aligned}$$

*Lemma 2* [28]: Suppose that there exists a matrix  $M \in \mathbb{R}^{n \times n}$  satisfying that  $\begin{bmatrix} R & * \\ M & R \end{bmatrix} \geq 0$  for given symmetric positive definite matrices  $R \in \mathbb{R}^{n \times n}$ . Then, for any scalar  $\theta \in (0, 1)$ , the following inequality holds:

$$\begin{bmatrix} \frac{1}{\theta}R & 0 \\ 0 & \frac{1}{1-\theta}R \end{bmatrix} \geq \begin{bmatrix} R & * \\ M & R \end{bmatrix}. \quad (17)$$

The aim of this paper is to design the hybrid-driven-based controllers (2) for NCCS (14), such that, in the presence of actuator saturations (12) and stochastic cyber attacks (15), the NCCS (14) is mean-square asymptotically stable, and  $\mathcal{H}_\infty$  performance constraint is satisfied. More specifically, the following requirements are satisfied.

- 1) The NCCS (14) with  $\omega(t) = 0$  is asymptotically stable in the mean-square sense.
- 2) Under the zero-initial condition, the inequality  $\mathbb{E}\{\int_0^\infty \|y_1(s)\|^2 ds\} < \gamma^2 \mathbb{E}\{\int_0^\infty \|\omega(s)\|^2 ds\}$  holds for all nonzero  $\omega(t) \in \mathcal{L}_2[0, \infty)$  and prescribed scalar  $\gamma > 0$ .

### III. MAIN RESULTS

In this section, the stability conditions for system (14) will be derived based on the Lyapunov–Krasovskii function method and the state feedback controllers (2) will be designed by means of LMI-based approaches [29]. The research results are stated as follows.

*Theorem 1:* For given positive scalars  $\bar{\alpha}$ ,  $\bar{\beta}$ ,  $\gamma$ , and  $0 < \varepsilon < 1$ , the upper bound of time-delays  $\eta_M > 0$ ,  $d_M > 0$ ,  $\tau_M > 0$ , and  $\theta_M > 0$ , trigger parameter  $\lambda$ , and matrices  $F$ ,  $K_1$ , and  $K_2$ , the system (14) is asymptotically stable in the mean-square sense if there exist matrices  $P_1 > 0$ ,  $P_2 > 0$ ,  $Q_i > 0$ ,  $R_i > 0$  ( $i = 1, 2, 3, 4$ ),  $\Omega > 0$ , and  $M_i$ ,  $N_i$ ,  $S_i$ ,  $W_i$  ( $i = 1, 2, 3, 4$ ) with appropriate dimensions such that

$$\Phi = \begin{bmatrix} \Phi_1 & * \\ \Phi_2 & \Phi_3 \end{bmatrix} < 0 \quad (18)$$

$$\Theta_i = \begin{bmatrix} R_i & * & * & * \\ 0 & 3R_i & * & * \\ U_{i1} & U_{i2} & R_i & * \\ U_{i3} & U_{i4} & 0 & 3R_i \end{bmatrix} \geq 0, i = 1, 2, 3, 4 \quad (19)$$

where

$$U_1 = M, \quad U_2 = N, \quad U_3 = S, \quad U_4 = W$$

$$\Phi_1 = \begin{bmatrix} \Phi_{11} & * & * & * & * & * & * & * \\ \Psi_1 & \Psi_{11} & * & * & * & * & * & * \\ \Psi_2 & 0 & \Psi_{22} + \lambda\Omega & * & * & * & * & * \\ \Psi_3 & 0 & 0 & \Psi_{33} & * & * & * & * \\ \Phi_{12} & \Phi_{13} & \Phi_{14} & 0 & \Phi_{15} & * & * & * \\ 0 & 0 & 0 & 0 & \Psi_4 & \Psi_{44} & * & * \\ \Phi_{16} & 0 & 0 & 0 & \Phi_{17} & 0 & \Phi_{18} & * \end{bmatrix}$$

$$\Phi_{11} = \text{sym}(P_1 A_1) + \sum_{j=1}^3 (Q_j - 4R_j), \quad \Phi_{12} = C_2^T B_1^T P_1$$

$$\Phi_{13} = [\bar{\beta}_1 \bar{\alpha} P_2 B_2 K_1 \quad 0 \quad 0 \quad 0], \quad \bar{\beta}_1 = 1 - \bar{\beta}$$

$$\Phi_{14} = [\bar{\beta}_1 \bar{\alpha}_1 P_2 B_2 K_1 \quad 0 \quad 0 \quad 0], \quad \bar{\alpha}_1 = 1 - \bar{\alpha}$$

$$\Phi_{15} = \text{sym}(P_2 A_2 + P_2 B_2 K_2) + Q_4 - 4R_4$$

$$\Phi_{16} = [0 \quad 0 \quad 0 \quad \Upsilon_3]^T, \quad \Upsilon_3 = P_1 B_1 D_2$$

$$\Phi_{17} = [\bar{\beta}_1 \bar{\alpha}_1 P_2 B_2 K_1 \quad \bar{\beta} P_2 B_2 K_1 \quad -P_2 B_2 \quad P_2 B_3]^T$$

$$\Phi_{18} = \text{diag}\{-\Omega, -\bar{\beta}I, -I, -\gamma^2 I\}$$

$$\Psi_i = \begin{bmatrix} -2R_i^T - \sum_{j=1}^4 U_{ij}^T & \Psi_{i2}^T & 6R_i^T & 2U_{i3}^T + 2U_{i4}^T \end{bmatrix}^T$$

$$\Psi_{i2}^T = U_{i1}^T + U_{i2}^T - U_{i3}^T - U_{i4}^T, \quad i = 1, 2, 3, 4$$

$$\Psi_{ii}^T = \begin{bmatrix} \Xi_{i1} & * & * & * \\ \Xi_{i2} & -Q_i - 4R_i & * & * \\ \Xi_{i3} & -2U_{i2}^T + 2U_{i4}^T & -12R_i & * \\ \Xi_{i4} & 6R_i & -4U_{i4} & -12R_i \end{bmatrix}$$

$$\Xi_{i1} = -8R_i + \text{sym}(U_{i1} - U_{i2} + U_{i3} - U_{i4})$$

$$\Xi_{i2} = -2R_i - U_{i1} + U_{i2} + U_{i3} - U_{i4}$$

$$\Xi_{i3} = 6R_i + 2U_{i2}^T + 2U_{i4}^T, \quad \Xi_{i4} = 6R_i - 2U_{i3} + 2U_{i4}$$

$$\Upsilon_1 = P_2 B_2 K_1, \quad \Upsilon_2 = P_2 B_2 K_2, \quad \sigma = \sqrt{\bar{\alpha}\bar{\alpha}_1}, \quad \delta = \sqrt{\bar{\beta}\bar{\beta}_1}$$

$$\Phi_2 = \begin{bmatrix} \Phi_{21} & \Phi_{22} & \Phi_{23} \\ \Phi_{24} & \Phi_{25} & \Phi_{26} \\ \Phi_{27} & \Phi_{28} & \Phi_{29} \end{bmatrix}, \quad \Phi_3 = \text{diag}\{\Phi_{31}, \Phi_{32}, \Phi_{33}\}$$

$$\Phi_{21} = \begin{bmatrix} \eta_M P_1 A_1 & 0_{1 \times 8} \\ d_M P_1 A_1 & 0_{1 \times 8} \\ \tau_M P_1 A_1 & 0_{1 \times 8} \end{bmatrix}, \quad \Phi_{23} = \begin{bmatrix} 0_{1 \times 3} & \eta_M \Upsilon_3 \\ 0_{1 \times 3} & d_M \Upsilon_3 \\ 0_{1 \times 3} & \tau_M \Upsilon_3 \end{bmatrix}$$

$$\Phi_{22} = \begin{bmatrix} 0_{1 \times 4} & \eta_M P_1 B_1 C_2 & 0_{1 \times 4} \\ 0_{1 \times 4} & d_M P_1 B_1 C_2 & 0_{1 \times 4} \\ 0_{1 \times 4} & \tau_M P_1 B_1 C_2 & 0_{1 \times 4} \end{bmatrix}$$

$$\Phi_{24} = \begin{bmatrix} 0 & \bar{\beta}_1 \bar{\alpha} \theta_M \Upsilon_1 & 0_{1 \times 3} & \bar{\beta}_1 \bar{\alpha}_1 \theta_M \Upsilon_1 & 0_{1 \times 3} \\ 0 & \sigma \bar{\beta}_1 \theta_M \Upsilon_1 & 0_{1 \times 3} & -\sigma \bar{\beta}_1 \theta_M \Upsilon_1 & 0_{1 \times 3} \\ 0 & -\delta \bar{\alpha} \theta_M \Upsilon_1 & 0_{1 \times 3} & -\delta \bar{\alpha}_1 \theta_M \Upsilon_1 & 0_{1 \times 3} \\ 0 & -\sigma \delta \theta_M \Upsilon_1 & 0_{1 \times 3} & \sigma \delta \theta_M \Upsilon_1 & 0_{1 \times 3} \end{bmatrix}$$

$$\Phi_{25} = \begin{bmatrix} 0_{1 \times 4} & \theta_M P_2 A_2 + \theta_M \Upsilon_2 & \theta_M P_2 A_3 & 0_{1 \times 3} \\ 0_{1 \times 4} & 0 & 0 & 0_{1 \times 3} \\ 0_{1 \times 4} & 0 & 0 & 0_{1 \times 3} \\ 0_{1 \times 4} & 0 & 0 & 0_{1 \times 3} \end{bmatrix}$$

$$\Phi_{26} = \begin{bmatrix} \bar{\beta}_1 \bar{\alpha}_1 \theta_M \Upsilon_1 & \bar{\beta} \theta_M \Upsilon_1 & -\theta_M P_2 B_2 & \theta_M P_2 B_3 \\ -\sigma \bar{\beta}_1 \theta_M \Upsilon_1 & 0 & 0 & 0 \\ -\delta \bar{\alpha}_1 \theta_M \Upsilon_1 & \delta \theta_M \Upsilon_1 & 0 & 0 \\ \sigma \delta \theta_M \Upsilon_1 & 0 & 0 & 0 \end{bmatrix}$$

$$\Phi_{27} = \begin{bmatrix} 0 & 0 & 0_{1 \times 3} & 0 & 0_{1 \times 3} \\ 0 & \sqrt{\varepsilon} \bar{\beta}_1 \bar{\alpha} K_1 & 0_{1 \times 3} & \sqrt{\varepsilon} \bar{\beta}_1 \bar{\alpha}_1 K_1 & 0_{1 \times 3} \\ 0 & \sqrt{\varepsilon} \bar{\beta}_1 \sigma K_1 & 0_{1 \times 3} & -\sqrt{\varepsilon} \bar{\beta}_1 \sigma K_1 & 0_{1 \times 3} \\ 0 & -\sqrt{\varepsilon} \bar{\alpha} \delta K_1 & 0_{1 \times 3} & -\sqrt{\varepsilon} \bar{\alpha}_1 \delta K_1 & 0_{1 \times 3} \\ 0 & -\sqrt{\varepsilon} \sigma \delta K_1 & 0_{1 \times 3} & \sqrt{\varepsilon} \sigma \delta K_1 & 0_{1 \times 3} \\ C_1 & 0 & 0_{1 \times 3} & 0 & 0_{1 \times 3} \end{bmatrix}$$

$$\Phi_{28} = \begin{bmatrix} \sqrt{\bar{\beta}} F & 0_{1 \times 3} & 0 & 0_{1 \times 4} \\ 0 & 0_{1 \times 3} & \sqrt{\varepsilon} K_2 & 0_{1 \times 4} \\ 0 & 0_{1 \times 3} & 0 & 0_{1 \times 4} \\ 0 & 0_{1 \times 3} & 0 & 0_{1 \times 4} \\ 0 & 0_{1 \times 3} & 0 & 0_{1 \times 4} \\ 0 & 0_{1 \times 3} & 0 & 0_{1 \times 4} \end{bmatrix}$$

$$\Phi_{29} = \begin{bmatrix} 0 & 0 & 0 & 0 \\ \sqrt{\varepsilon} \bar{\beta}_1 \bar{\alpha}_1 K_1 & \sqrt{\varepsilon} \bar{\beta} K_1 & 0 & 0 \\ -\sqrt{\varepsilon} \bar{\beta}_1 \sigma K_1 & 0 & 0 & 0 \\ -\sqrt{\varepsilon} \bar{\alpha}_1 \delta K_1 & \sqrt{\varepsilon} \delta K_1 & 0 & 0 \\ \sqrt{\varepsilon} \sigma \delta K_1 & 0 & 0 & 0 \\ 0 & 0 & 0 & D_1 \end{bmatrix}$$

$$\Phi_{31} = \text{diag}\{-P_1 R_1^{-1} P_1, -P_1 R_2^{-1} P_1, -P_1 R_3^{-1} P_1\}$$

$$\Phi_{32} = \text{diag}\{-P_2 R_4^{-1} P_2, -P_2 R_4^{-1} P_2, -P_2 R_4^{-1} P_2 - P_2 R_4^{-1} P_2\}$$

$$\Phi_{33} = \text{diag}\{-I, -I, -I, -I, -I, -I\}.$$

*Proof:* See Appendix A. ■

Theorem 1 presents the sufficient conditions, which guarantee the asymptotical stability of the system (14) in the

mean-square sense. Based on the results in Theorem 1, the following theorem is devoted to designing the controllers in the form of (2).

*Theorem 2:* For given positive scalars  $\bar{\alpha}$ ,  $\bar{\beta}$ ,  $\eta_M$ ,  $d_M$ ,  $\tau_M$ ,  $\theta_M$ ,  $\lambda$ ,  $\varepsilon$ ,  $\gamma$ ,  $\varepsilon_1$ ,  $\varepsilon_2$ ,  $\varepsilon_3$ ,  $\varepsilon_4$ , and  $\varepsilon_f$  and matrix  $F$ , the system (14) is mean-square asymptotically stable if there exist positive matrices  $X_1 > 0$ ,  $X_2 > 0$ ,  $\tilde{Q}_1 > 0$ ,  $\tilde{Q}_2 > 0$ ,  $\tilde{Q}_3 > 0$ ,  $\tilde{Q}_4 > 0$ ,  $\tilde{R}_1 > 0$ ,  $\tilde{R}_2 > 0$ ,  $\tilde{R}_3 > 0$ ,  $\tilde{R}_4 > 0$ ,  $\tilde{\Omega} > 0$ ,  $\tilde{M}_i$ ,  $\tilde{N}_i$ ,  $\tilde{S}_i$ ,  $\tilde{W}_i$  ( $i = 1, 2, 3, 4$ ), and  $Y_1$ ,  $Y_2$  with appropriate dimensions such that the following LMIs hold

$$\tilde{\Phi} = \begin{bmatrix} \tilde{\Phi}_1 & * \\ \tilde{\Phi}_2 & \tilde{\Phi}_3 \end{bmatrix} < 0 \quad (20)$$

$$\tilde{\Theta}_i = \begin{bmatrix} \tilde{R}_i & * & * & * \\ 0 & 3\tilde{R}_i & * & * \\ \tilde{U}_{i1} & \tilde{U}_{i2} & \tilde{R}_i & * \\ \tilde{U}_{i3} & \tilde{U}_{i4} & 0 & 3\tilde{R}_i \end{bmatrix} \geq 0, i = 1, 2, 3 \quad (21)$$

$$\hat{\Theta}_4 = \begin{bmatrix} \hat{R}_4 & * & * & * \\ 0 & 3\hat{R}_4 & * & * \\ \hat{W}_1 & \hat{W}_2 & \hat{R}_4 & * \\ \hat{W}_3 & \hat{W}_4 & 0 & 3\hat{R}_4 \end{bmatrix} \geq 0 \quad (22)$$

where  $\tilde{\Phi}$ ,  $\tilde{\Theta}_i$  ( $i = 1, 2, 3$ ), and  $\hat{\Theta}_4$  are, respectively, derived from  $\Phi$ ,  $\Theta_i$  ( $i = 1, 2, 3$ ), and  $\Theta_4$  by substitute  $U_i$  ( $i = 1, 2, 3$ ),  $W$ ,  $\Omega$ ,  $R_i$  ( $i = 1, 2, 3$ ),  $R_4$ ,  $P_1A_1$ ,  $P_1B_1$ ,  $P_2A_2$ ,  $P_2B_2$ ,  $P_2A_3$ ,  $P_2B_3$ ,  $C_1$ ,  $F$ ,  $K_1$ ,  $K_2$ ,  $\tilde{\beta}I$ ,  $-P_1R_i^{-1}P_1$  ( $i = 1, 2, 3$ ), and  $-P_2R_4^{-1}P_2$  with  $\tilde{U}_i$  ( $i = 1, 2, 3$ ),  $\tilde{W}$ ,  $\tilde{\Omega}$ ,  $\tilde{R}_i$  ( $i = 1, 2, 3$ ),  $\hat{R}_4$ ,  $A_1X_1$ ,  $B_1$ ,  $A_2X_2$ ,  $B_2$ ,  $A_3X_2$ ,  $B_3$ ,  $C_1X_1$ ,  $FX_1$ ,  $Y_1$ ,  $Y_2$ ,  $-2\tilde{\beta}\varepsilon_fX_1 + \tilde{\beta}\varepsilon_f^2I$ ,  $-2\varepsilon_iX_1 + \varepsilon_i^2\tilde{R}_i$  ( $i = 1, 2, 3$ ), and  $-2\varepsilon_4X_2 + \varepsilon_4^2\hat{R}_4$  accordingly. Other symbols have been defined in Theorem 1.

Moreover, the desired state feedback gain of primary controller is given by

$$K_1 = Y_1X_1^{-1} \quad (23)$$

and the desired state feedback gain of secondary controller is given by

$$K_2 = Y_2X_2^{-1}. \quad (24)$$

*Proof:* See Appendix B. ■

#### IV. SIMULATION EXAMPLES

In this section, a simulation example is given to illustrate the usefulness of the proposed approach in this paper. The example is based on a power plant gas-turbine system, the schematic diagram of which is shown in Fig. 2, where the turbine is driven by superheated gas. It should be pointed that the proper temperature of superheated gas plays an especially important role in ensuring the turbine work successfully. In the gas generation process, the three-way plug valve receives air from blower and then send it to two sides. On the one hand, the air functions as a combustion improver in the burning of fuel oil to generate superheated gas. On the other hand, the air takes for cooling the superheated gas.

In order to generate superheated gas with proper temperature, the networked cascade control is adopted, where the outlet gas temperature and the cooling air temperature are measured by primary sensor  $Sensor_1$  and secondary sensor

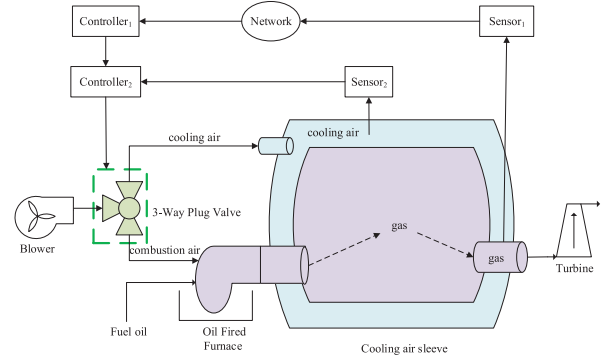


Fig. 2. Schematic of NCCS for gas-turbine system.

$Sensor_2$ , respectively. The communication between  $Sensor_1$  and primary controller  $Controller_1$  relies on a network, and the output of  $Controller_1$  is the input of the secondary controller  $Controller_2$ , which controls the three-way-plus-valve to modulate the two-side air output and thus the proper gas temperature can be guaranteed.

Consider the power plant gas-turbine system [7] with state-space representation of the primary plant (1) as

$$\begin{cases} \dot{x}_1(t) = \begin{bmatrix} -1 & 0 \\ -1 & -2 \end{bmatrix} x_1(t) + \begin{bmatrix} 2 \\ 0.1 \end{bmatrix} y_2(t) \\ y_1(t) = \begin{bmatrix} 0 & 0.1 \end{bmatrix} x_1(t) + 0.2\omega(t) \end{cases}$$

and the state-space representation of the secondary plant (9) as

$$\begin{cases} \dot{x}_2(t) = \begin{bmatrix} 1.3 & 1 \\ 0.2 & 0 \end{bmatrix} x_2(t) + \begin{bmatrix} 0.2 & 0.1 \\ 0.2 & 1 \end{bmatrix} x_2(t - \theta(t)) \\ \quad + \begin{bmatrix} 0.2 \\ 1 \end{bmatrix} \text{sat}(u_2(t)) + \begin{bmatrix} -0.4 \\ 0.1 \end{bmatrix} \omega(t) \\ y_2(t) = \begin{bmatrix} -0.3 & 0.1 \end{bmatrix} x_2(t) + 0.1\omega(t). \end{cases}$$

The initial states of the two plants are given as  $x_{10} = [-3 \ 0]^T$  and  $x_{20} = [-1 \ 1]^T$ .

The external disturbance is assumed as

$$\omega(t) = \begin{cases} 0.1 \sin(2\pi t), & 0 \leq t \leq 10 \\ 0, & \text{otherwise.} \end{cases}$$

The nonlinear signal of cyber attacks is chosen as

$$f(x_1(t)) = \begin{bmatrix} -\tanh(0.02x_{11}(t)) \\ -\tanh(0.1x_{12}(t)) \end{bmatrix}.$$

It can be seen from Assumption 1 that when the nonlinearity bound is specified as  $F = \text{diag}\{0.02, 0.1\}$ , the condition (15) can be guaranteed.

In the following, by taking the actuator saturations and stochastic cyber attacks into consideration, three possible cases concerning the different schemes of data transmission, which is indicated by the random variable  $\alpha(t)$ , will be presented to illustrate the usefulness of designed  $\mathcal{H}_\infty$  state feedback controllers.

*Case 1:* Given  $\bar{\alpha} = 0.25$ , the data from primary sensor to primary controller is transmitted via hybrid triggered scheme. Choose sampling period  $h = 0.1$  s, and assume scalars as  $\bar{\beta} = 0.02$ ,  $\eta_M = 0.5$ ,  $d_M = 0.5$ ,  $\tau_M = 0.2$ ,  $\theta_M = 0.2$ ,  $\lambda = 0.16$ ,  $\varepsilon = 0.2$ ,  $\gamma = 2$ , and  $\varepsilon_1 = \varepsilon_2 = \varepsilon_3 = \varepsilon_4 = \varepsilon_f = 1$ .

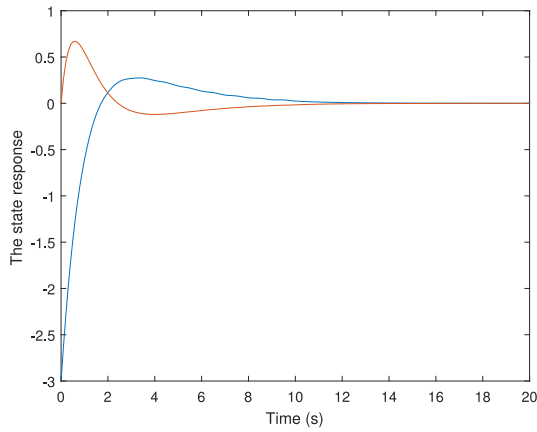


Fig. 3. State responses of primary plant in case 1.

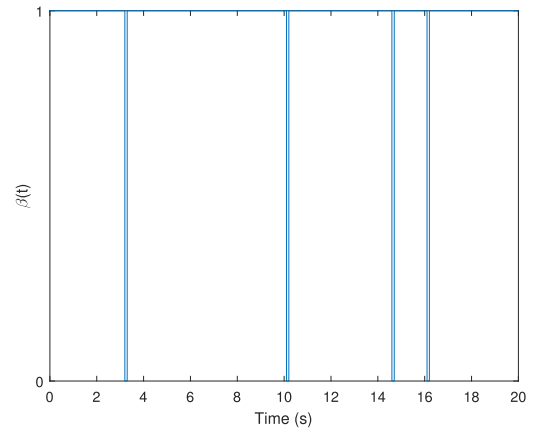


Fig. 6.  $\beta(t)$  with  $\bar{\beta} = 0.02$  in case 1.

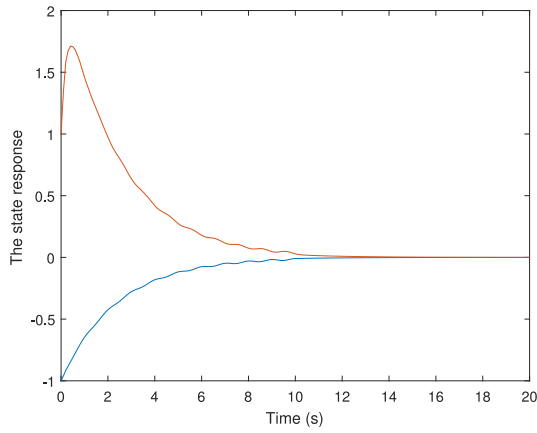


Fig. 4. State responses of secondary plant in case 1.

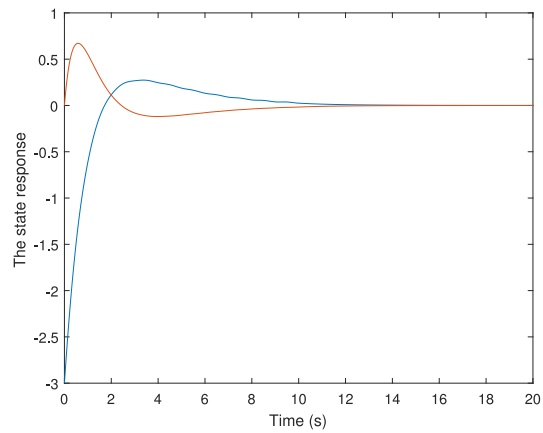


Fig. 7. State responses of primary plant in case 2.

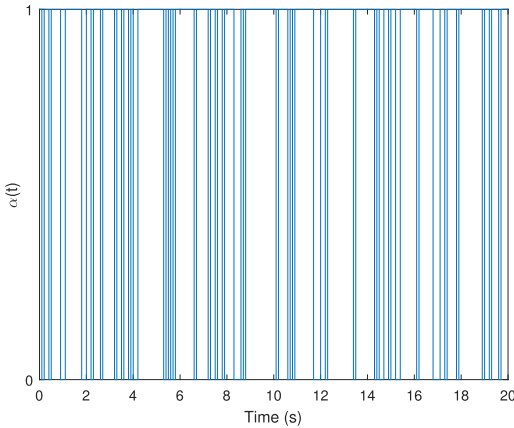


Fig. 5.  $\alpha(t)$  with  $\bar{\alpha} = 0.25$  in case 1.

By applying Theorem 2, the gains of state feedback controllers are achieved as  $K_1 = [-0.0066 \ 0.0002]$  and  $K_2 = [-11.1586 \ -6.1972]$  and event-triggered matrix is  $\Omega = \begin{bmatrix} 0.1181 & 0.0539 \\ 0.0539 & 0.1587 \end{bmatrix}$ . The state responses of primary plant and secondary plant with actuator saturations and stochastic cyber attacks are shown in Figs. 3 and 4, respectively. The Bernoulli distribution random variable  $\alpha(t)$  is depicted in Fig. 5, which is introduced to indicate the switch rule in hybrid triggered

scheme. In addition,  $\beta(t)$  governing the occurrence of cyber attacks is shown in Fig. 6 with given expectation.

*Case 2:* When  $\bar{\alpha} = 1$ , the data transmission from primary sensor to primary controller is implemented by time-triggered scheme. Choose sampling period  $h = 0.01$  s, and for given  $\bar{\beta} = 0.02$ ,  $\eta_M = 0.5$ ,  $d_M = 0.5$ ,  $\tau_M = 0.2$ ,  $\theta_M = 0.2$ ,  $\lambda = 0$ ,  $\varepsilon = 0.2$ ,  $\gamma = 2$ , and  $\epsilon_1 = \epsilon_2 = \epsilon_3 = \epsilon_4 = \epsilon_f = 1$ . According to Theorem 2, the controller feedback gains are calculated as  $K_1 = [-0.0125 \ -0.0009]$  and  $K_2 = [-11.1506 \ -6.2001]$ . Figs. 7 and 8 show the state responses of primary plant and secondary plant, respectively. The saturation control signal  $\text{sat}(u_2(t))$  is depicted in Fig. 9 with red solid line while the original control signal is with blue dashed.

*Case 3:* If  $\bar{\alpha} = 0$ , the data transmission from primary sensor to primary controller is under event-triggered scheme. Choose sampling period  $h = 0.1$ s, and set  $\bar{\beta} = 0.02$ ,  $\eta_M = 0.5$ ,  $d_M = 0.5$ ,  $\tau_M = 0.2$ ,  $\theta_M = 0.2$ ,  $\lambda = 0.16$ ,  $\varepsilon = 0.2$ ,  $\gamma = 2$ , and  $\epsilon_1 = \epsilon_2 = \epsilon_3 = \epsilon_4 = \epsilon_f = 1$ . By using Theorem 2, the gains of state feedback controllers are obtained as  $K_1 = [-0.0101 \ -0.0009]$  and  $K_2 = [-11.1411 \ -6.1938]$  and event-triggered matrix is  $\Omega = \begin{bmatrix} 0.1178 & 0.0538 \\ 0.0538 & 0.1584 \end{bmatrix}$ . The state responses of the primary plant and secondary plant with actuator saturations and stochastic cyber attacks are presented in

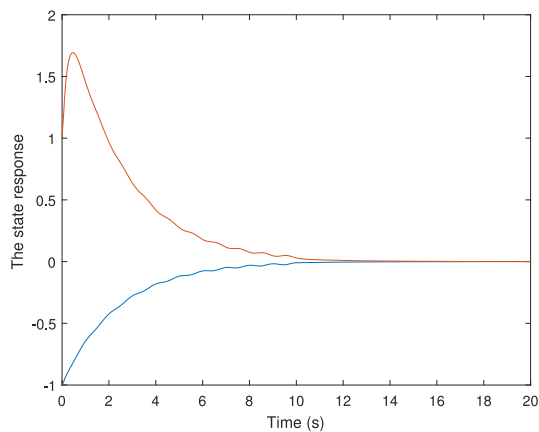


Fig. 8. State responses of secondary plant in case 2.

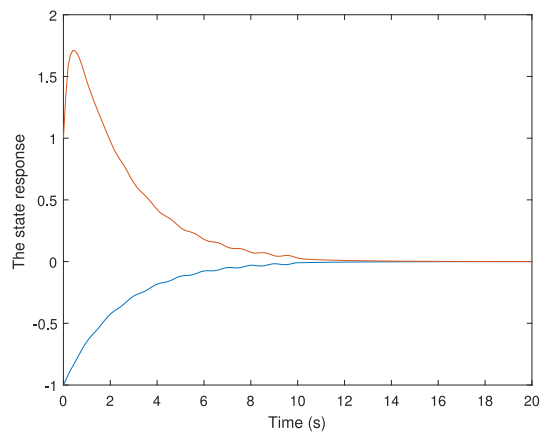


Fig. 11. State responses of secondary plant in case 3.

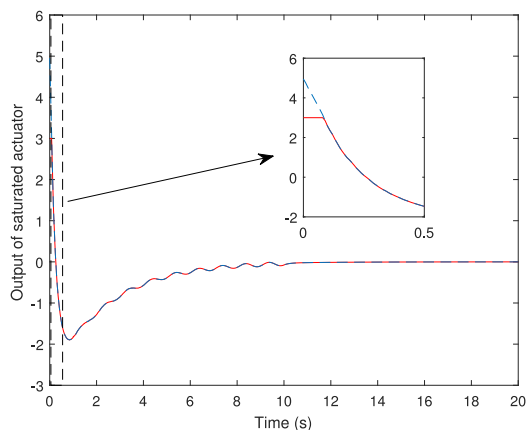


Fig. 9. Output of saturated actuator in case 2.

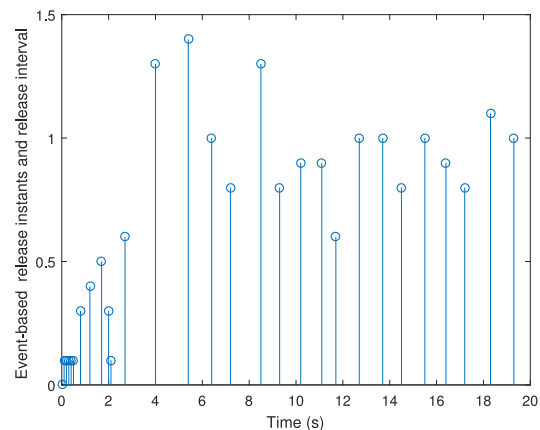


Fig. 12. Release instants and release interval in case 3.

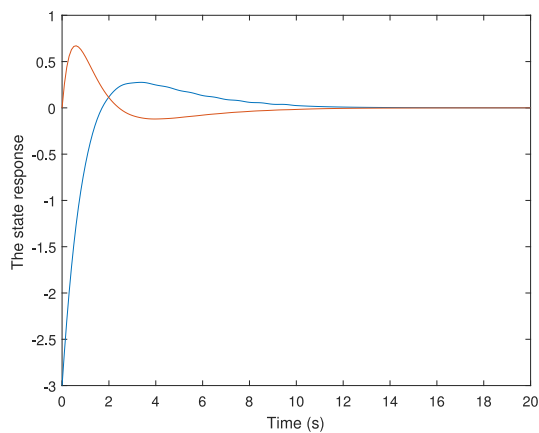


Fig. 10. State responses of primary plant in case 3.

Figs. 10 and 11, respectively. The communication instants and communication intervals are given in Fig. 12.

According to Theorem 2, the gain matrices of  $\mathcal{H}_\infty$  primary and secondary controllers as well as the event-triggered matrix can be calculated. Figs. 3, 4, 7, 8, 10, and 11 show the state responses under different situations, which illustrate that the system can be stabilized by the design approach proposed in this paper. From the figures of state responses above, it can be easily seen that the system performance is degraded by

actuator saturations and stochastic cyber attacks. Fig. 12 shows that the transmission frequency is degraded obviously by using event-triggered scheme. Consequently, the burden of network bandwidth can be reduced significantly.

### V. CONCLUSION

This paper addresses the issue about  $\mathcal{H}_\infty$  control for hybrid-driven-based NCCSs with actuator saturations and stochastic cyber attacks. A hybrid triggered scheme is introduced to reduce the burden of network bandwidth, where a Bernoulli distribution random variable is utilized to describe the switching rule between the time-triggered scheme and the event-triggered scheme. By taking hybrid triggered scheme, stochastic cyber attacks and actuator saturations into account, a new model for NCCSs is established. Sufficient conditions for the stability of the NCCS are derived by employing Lyapunov stability theory. Moreover, the state feedback gains of both primary controller and secondary controller are obtained in terms of LMI techniques. The simulation example confirms the usefulness of the designed state feedback controllers when considering hybrid triggered scheme, actuator saturations, and stochastic cyber attacks. In our future research, the functional observers will be designed to detect and isolate those attacks in order to make the controller further robust against the cyber attacks.



APPENDIX A  
PROOF OF THEOREM 1

Choose a Lyapunov–Krasovskii functional candidate for system (14)

$$V(t) = V_1(t) + V_2(t) + V_3(t) \quad (25)$$

where

$$\begin{aligned} V_1(t) &= x_1^T(t)P_1x_1(t) + x_2^T(t)P_2x_2(t) \\ V_2(t) &= \sum_{i=1}^3 \int_{t-r_i}^t x_1^T(s)Q_i x_1(s) ds \\ &\quad + \int_{t-\theta_M}^t x_2^T(s)Q_4 x_2(s) ds \\ V_3(t) &= \sum_{i=1}^3 r_i \int_{t-r_i}^t \int_s^t \dot{x}_1^T(v)R_i \dot{x}_1(v) dv ds \\ &\quad + \theta_M \int_{t-\theta_M}^t \int_s^t \dot{x}_2^T(v)R_4 \dot{x}_2(v) dv ds \end{aligned}$$

and  $r_1 = \eta_M$ ,  $r_2 = d_M$ ,  $r_3 = \eta_M$ ,  $Q_j > 0$ , and  $R_j > 0$  ( $j = 1, 2, 3, 4$ ).

By taking derivation and expectation on  $V_i(t)$  ( $i = 1, 2, 3$ ), it can be obtained that

$$\mathbb{E}\{\dot{V}_1(t)\} = 2x_1^T(t)P_1\dot{x}_1(t) + 2\mathbb{E}\{x_2^T(t)P_2\dot{x}_2(t)\} \quad (26)$$

$$\begin{aligned} \mathbb{E}\{\dot{V}_2(t)\} &= \sum_{i=1}^3 x_1^T(t)Q_i x_1(t) + x_2^T(t)Q_4 x_2(t) \\ &\quad - \sum_{i=1}^3 x_1^T(t-r_i)Q_i x_1(t-r_i) \\ &\quad - x_2^T(t-\theta_M)Q_4 x_2(t-\theta_M) \end{aligned} \quad (27)$$

$$\begin{aligned} \mathbb{E}\{\dot{V}_3(t)\} &= \dot{x}_1^T(t)(\eta_M^2 R_1 + d_M^2 R_2 + \tau_M^2 R_3)\dot{x}_1(t) \\ &\quad + \mathbb{E}\left\{\dot{x}_2^T(t)\theta_M^2 R_4 \dot{x}_2(t)\right\} \\ &\quad - \theta_M \int_{t-\theta_M}^t \dot{x}_2^T(v)R_4 \dot{x}_2(v) dv \\ &\quad - \sum_{i=1}^3 r_i \int_{t-r_i}^t \dot{x}_1^T(v)R_i \dot{x}_1(v) dv. \end{aligned} \quad (28)$$

Notice that

$$2\mathbb{E}\{x_2^T(t)P_2\dot{x}_2(t)\} = 2x_2^T(t)P_2[\mathbb{A}_0 + \mathbb{A}_1]$$

where

$$\begin{aligned} \mathbb{A}_0 &= (A_2 + B_2 K_2)x_2(t) + A_3 x_2(t - \theta(t)) \\ &\quad - B_2 \phi(u_2(t)) + B_3 \omega(t) \\ \mathbb{A}_1 &= (1 - \bar{\beta})\bar{\alpha} B_2 K_1 x_1(t - \eta(t)) \\ &\quad + (1 - \bar{\beta})(1 - \bar{\alpha})B_2 K_1 x_1(t - d(t)) \\ &\quad + (1 - \bar{\beta})(1 - \bar{\alpha})B_2 K_1 e_k(t) \\ &\quad + \bar{\beta} B_2 K_1 f(x_1(t - \tau(t))) \end{aligned}$$

since the random variables  $\alpha(t)$  and  $\beta(t)$  are assumed to be uncorrelated to each other and  $\mathbb{E}\{\alpha(t)\} = \bar{\alpha}$ ,  $\mathbb{E}\{\beta(t)\} = \bar{\beta}$ .

Notice that

$$\begin{aligned} \dot{x}_2(t) &= \mathcal{A}_0 + (\alpha(t) - \bar{\alpha})\mathcal{A}_1 + (\beta(t) - \bar{\beta})\mathcal{A}_2 \\ &\quad + (\alpha(t) - \bar{\alpha})(\beta(t) - \bar{\beta})\mathcal{A}_3 \end{aligned}$$

where

$$\begin{aligned} \mathcal{A}_0 &= \mathbb{A}_0 + \bar{\beta} B_2 K_1 f(x_1(t - \tau(t))) + (1 - \bar{\beta})\mathbb{A}_2 \\ \mathcal{A}_1 &= (1 - \bar{\beta})\mathbb{A}_3, \quad \mathcal{A}_3 = -\mathbb{A}_3 \\ \mathcal{A}_2 &= B_2 K_1 f(x_1(t - \tau(t))) - \mathbb{A}_2 \\ \mathbb{A}_2 &= \bar{\alpha} B_2 K_1 x_1(t - \eta(t)) + (1 - \bar{\alpha})B_2 K_1 x_1(t - d(t)) \\ &\quad + (1 - \bar{\alpha})B_2 K_1 e_k(t) \\ \mathbb{A}_3 &= B_2 K_1 x_1(t - \eta(t)) - B_2 K_1 x_1(t - d(t)) \\ &\quad - B_2 K_1 e_k(t). \end{aligned}$$

Furthermore

$$\begin{aligned} \mathbb{E}\{\alpha(t) - \bar{\alpha}\} &= 0, \quad \mathbb{E}\{(\alpha(t) - \bar{\alpha})^2\} = \sigma^2 \\ \mathbb{E}\{\beta(t) - \bar{\beta}\} &= 0, \quad \mathbb{E}\{(\beta(t) - \bar{\beta})^2\} = \delta^2. \end{aligned}$$

Therefore

$$\begin{aligned} \mathbb{E}\left\{\dot{x}_2^T(t)\theta_M^2 R_4 \dot{x}_2(t)\right\} &= \mathcal{A}_0^T \theta_M^2 R_4 \mathcal{A}_0 + \sigma^2 \mathcal{A}_1^T \theta_M^2 R_4 \mathcal{A}_1 \\ &\quad + \delta^2 \mathcal{A}_2^T \theta_M^2 R_4 \mathcal{A}_2 + \sigma^2 \delta^2 \mathcal{A}_3^T \theta_M^2 R_4 \mathcal{A}_3. \end{aligned} \quad (29)$$

Define

$$\begin{aligned} \varrho_1 &= [x_1^T(t - \eta(t)) \quad x_1^T(t - \eta_M) \quad \varrho_{11}]^T \\ \varrho_2 &= [x_1^T(t - d(t)) \quad x_1^T(t - d_M) \quad \varrho_{22}]^T \\ \varrho_3 &= [x_1^T(t - \tau(t)) \quad x_1^T(t - \tau_M) \quad \varrho_{33}]^T \\ \varrho_4 &= [x_2^T(t - \theta(t)) \quad x_2^T(t - \theta_M) \quad \varrho_{44}]^T \end{aligned}$$

where

$$\begin{aligned} \varrho_{11} &= \left[ \frac{1}{\eta(t)} \int_{t-\eta(t)}^t x_1^T(s) ds \quad \frac{1}{\eta_M - \eta(t)} \int_{t-\eta_M}^{t-\eta(t)} x_1^T(s) ds \right] \\ \varrho_{22} &= \left[ \frac{1}{d(t)} \int_{t-d(t)}^t x_1^T(s) ds \quad \frac{1}{d_M - d(t)} \int_{t-d_M}^{t-d(t)} x_1^T(s) ds \right] \\ \varrho_{33} &= \left[ \frac{1}{\tau(t)} \int_{t-\tau(t)}^t x_1^T(s) ds \quad \frac{1}{\tau_M - \tau(t)} \int_{t-\tau_M}^{t-\tau(t)} x_1^T(s) ds \right] \\ \varrho_{44} &= \left[ \frac{1}{\theta(t)} \int_{t-\theta(t)}^t x_2^T(s) ds \quad \frac{1}{\theta_M - \theta(t)} \int_{t-\theta_M}^{t-\theta(t)} x_2^T(s) ds \right]. \end{aligned}$$

By employing Lemma 1, it can be derived easily that

$$\begin{aligned} & -\theta_M \int_{t-\theta(t)}^t \dot{x}_2^T(s)R_4 \dot{x}_2(s) ds \\ & \leq -\frac{\theta_M}{\theta(t)} \begin{bmatrix} \Pi_{41} \\ \Pi_{42} \end{bmatrix}^T \begin{bmatrix} R_4 & * \\ 0 & 3R_4 \end{bmatrix} \begin{bmatrix} \Pi_{41} \\ \Pi_{42} \end{bmatrix} \end{aligned} \quad (30)$$

$$\begin{aligned} & -\theta_M \int_{t-\theta_M}^{t-\theta(t)} \dot{x}_2^T(s)R_4 \dot{x}_2(s) ds \\ & \leq -\frac{\theta_M}{\theta_M - \theta(t)} \begin{bmatrix} \Pi_{43} \\ \Pi_{44} \end{bmatrix}^T \begin{bmatrix} R_4 & * \\ 0 & 3R_4 \end{bmatrix} \begin{bmatrix} \Pi_{43} \\ \Pi_{44} \end{bmatrix} \end{aligned} \quad (31)$$

where  $\Pi_{41} = x_2(t) - e_1 \varrho_4$ ,  $\Pi_{42} = x_2(t) + e_1 \varrho_4 - 2e_3 \varrho_4$ ,  $\Pi_{43} = e_1 \varrho_4 - e_2 \varrho_4$ ,  $\Pi_{44} = e_1 \varrho_4 + e_2 \varrho_4 - 2e_4 \varrho_4$ , and  $e_i$  ( $i = 1, 2, 3, 4$ ) are compatible row-block matrices with  $i$ th block of an identify matrix.

Then, the following bounding inequality can be obtained by applying Lemma 2 to (30) and (31):

$$-\theta_M \int_{t-\theta_M}^t \dot{x}_2^T(s) R_4 \dot{x}_2(s) ds \leq - \begin{bmatrix} \Pi_{41} \\ \Pi_{42} \\ \Pi_{43} \\ \Pi_{44} \end{bmatrix}^T \begin{bmatrix} R_4 & * & * & * \\ 0 & 3R_4 & * & * \\ W_1 & W_2 & R_4 & * \\ W_3 & W_4 & 0 & 3R_4 \end{bmatrix} \begin{bmatrix} \Pi_{41} \\ \Pi_{42} \\ \Pi_{43} \\ \Pi_{44} \end{bmatrix}. \quad (32)$$

Similarly, using Lemmas 1 and 2, we can get the estimation of the other integral terms in (28) as follows:

$$-\sum_{i=1}^3 r_i \int_{t-r_i}^t \dot{x}_1^T(s) R_i \dot{x}_1(s) ds \leq - \sum_{i=1}^3 \begin{bmatrix} \Pi_{i1} \\ \Pi_{i2} \\ \Pi_{i3} \\ \Pi_{i4} \end{bmatrix}^T \begin{bmatrix} R_i & * & * & * \\ 0 & 3R_i & * & * \\ U_{i1} & U_{i2} & R_i & * \\ U_{i3} & U_{i4} & 0 & 3R_i \end{bmatrix} \begin{bmatrix} \Pi_{i1} \\ \Pi_{i2} \\ \Pi_{i3} \\ \Pi_{i4} \end{bmatrix} \quad (33)$$

where  $U_1 = M$ ,  $U_2 = N$ ,  $U_3 = S$ ,  $\Pi_{i1} = x_1(t) - e_{1i} \varrho_i$ ,  $\Pi_{i2} = x_1(t) + e_{1i} \varrho_i - 2e_{3i} \varrho_i$ ,  $\Pi_{i3} = e_{1i} \varrho_i - e_{2i} \varrho_i$ , and  $\Pi_{i4} = e_{1i} \varrho_i + e_{2i} \varrho_i - 2e_{4i} \varrho_i$  ( $i = 1, 2, 3$ ).

By recalling the restricted condition (4), the triggering condition, which should be violated when transmitting the sampled data under event-triggered scheme, is as follows:

$$\lambda x_1^T(t-d(t)) \Omega x_1(t-d(t)) - e_k^T(t) \Omega e_k(t) \geq 0. \quad (34)$$

From Assumption 1, the following inequality condition can be obtained:

$$\bar{\beta} x_1^T(t-\tau(t)) F^T F x_1(t-\tau(t)) - \bar{\beta} f^T(x_1(t-\tau(t))) f(x_1(t-\tau(t))) \geq 0. \quad (35)$$

Reconsider the inequality (12) about nonlinear function  $\phi(u_2(t))$ , namely

$$\varepsilon u_2^T(t) u_2(t) - \phi^T(u_2(t)) \phi(u_2(t)) \geq 0. \quad (36)$$

Note that

$$u_2(t) = \mathcal{B}_0 + (\alpha(t) - \bar{\alpha}) \mathcal{B}_1 + (\beta(t) - \bar{\beta}) \mathcal{B}_2 + (\alpha(t) - \bar{\alpha})(\beta(t) - \bar{\beta}) \mathcal{B}_3$$

where

$$\begin{aligned} \mathcal{B}_0 &= (1 - \bar{\beta}) \bar{\alpha} K_1 x_1(t - \eta(t)) \\ &\quad + (1 - \bar{\beta})(1 - \bar{\alpha}) K_1 x_1(t - d(t)) \\ &\quad + K_2 x_2(t) + \bar{\beta} K_1 f(x_1(t - \tau(t))) \\ &\quad + (1 - \bar{\beta})(1 - \bar{\alpha}) K_1 e_k(t) \\ \mathcal{B}_1 &= (1 - \bar{\beta}) K_1 x_1(t - \eta(t)) + (1 - \bar{\beta}) K_1 x_1(t - d(t)) \\ &\quad + (1 - \bar{\beta}) K_1 e_k(t) \\ \mathcal{B}_2 &= -\bar{\alpha} K_1 x_1(t - \eta(t)) - (1 - \bar{\alpha}) K_1 x_1(t - d(t)) \\ &\quad + K_1 f(x_1(t - \tau(t))) - (1 - \bar{\alpha}) K_1 e_k(t) \\ \mathcal{B}_3 &= -K_1 x_1(t - \eta(t)) + K_1 x_1(t - d(t)) + K_1 e_k(t). \end{aligned}$$

Therefore, it is easy to get that

$$\mathbb{E}\{\varepsilon u_2^T(t) u_2(t)\} = \varepsilon \mathcal{B}_0^T \mathcal{B}_0 + \sigma^2 \varepsilon \mathcal{B}_1^T \mathcal{B}_1 + \delta^2 \varepsilon \mathcal{B}_2^T \mathcal{B}_2 + \sigma^2 \delta^2 \varepsilon \mathcal{B}_3^T \mathcal{B}_3. \quad (37)$$

Define  $\xi(t) = [x_1^T(t), \varrho_1^T, \varrho_2^T, \varrho_3^T, x_2^T(t), \varrho_4^T, e_k^T(t), f^T(x_1(t - \tau(t))), \phi^T(u_2(t)), \omega^T(t)]^T$ . By combining (26)–(37) and utilizing Schur complement lemma [30], it yields

$$\mathbb{E}\{\dot{V}(t)\} + \mathbb{E}\{y_1^T(t) y_1(t)\} - \gamma^2 \mathbb{E}\{\omega^T(t) \omega(t)\} < \xi^T(t) \Phi \xi(t). \quad (38)$$

Since  $\Phi < 0$  can be ensured by (18) and (19), it can be concluded from (38) that

$$\mathbb{E}\{\dot{V}(t)\} + \mathbb{E}\{y_1^T(t) y_1(t)\} - \gamma^2 \mathbb{E}\{\omega^T(t) \omega(t)\} < 0. \quad (39)$$

When  $\omega(t) = 0$ , (39) means  $\mathbb{E}\{\dot{V}(t)\} < 0$ . Due to  $V(t) > 0$ ,  $\mathbb{E}\{\dot{V}(t)\} < 0$ , it is easy to yield that  $\lim_{t \rightarrow \infty} \mathbb{E}\{\|\bar{x}(t)\|^2\} = 0$  for any initial conditions, where  $\bar{x}(t) = [x_1^T(t) \ x_2^T(t)]^T$ . Therefore, system (14) is mean-square asymptotically stable in the case of  $\omega(t) = 0$ .

When  $\omega(t)$  is nonzero, by integrating both sides of (39) from 0 to  $t$ , it can be derived that

$$V(t) - V(0) + \mathbb{E}\left\{\int_0^t y_1^T(s) y_1(s) ds\right\} - \gamma^2 \mathbb{E}\left\{\int_0^t \omega^T(s) \omega(s) ds\right\} < 0. \quad (40)$$

Letting  $t \rightarrow \infty$  and under the zero-initial condition, it can be obtained from (40) that

$$\mathbb{E}\left\{\int_0^\infty y_1^T(s) y_1(s) ds\right\} < \gamma^2 \mathbb{E}\left\{\int_0^\infty \omega^T(s) \omega(s) ds\right\} \quad (41)$$

which means the specified  $\mathcal{H}_\infty$  norm constraint is satisfied.

This completes the proof.

## APPENDIX B

### PROOF OF THEOREM 2

Due to  $(R_k - \varepsilon_k^{-1} P_1) R_k^{-1} (R_k - \varepsilon_k^{-1} P_1) \geq 0$ , ( $k = 1, 2, 3$ ), it can be obtained that

$$-P_1 R_k^{-1} P_1 \leq -2\varepsilon_k P_1 + \varepsilon_k^2 R_k, \quad (k = 1, 2, 3). \quad (42)$$

Similarly

$$-P_2 R_4^{-1} P_2 \leq -2\varepsilon_4 P_2 + \varepsilon_4^2 R_4 \quad (43)$$

and then

$$\bar{\Phi} < 0 \quad (44)$$

can guarantee (18) holds, where  $\bar{\Phi}$  is obtained by substituting the terms  $\Phi_{31}$  and  $\Phi_{32}$  with  $\bar{\Phi}_{31} = \text{diag}\{-2\varepsilon_1 P_1 + \varepsilon_1^2 R_1, -2\varepsilon_2 P_1 + \varepsilon_2^2 R_2, -2\varepsilon_3 P_1 + \varepsilon_3^2 R_3\}$  and  $\bar{\Phi}_{32} = \text{diag}\{-2\varepsilon_4 P_2 + \varepsilon_4^2 R_4, -2\varepsilon_4 P_2 + \varepsilon_4^2 R_4, -2\varepsilon_4 P_2 + \varepsilon_4^2 R_4, -2\varepsilon_4 P_2 + \varepsilon_4^2 R_4\}$ , respectively.

Define  $X_1 = P_1^{-1}$ ,  $X_2 = P_2^{-1}$ ,  $\tilde{Q}_j = X_1 Q_j X_1$ ,  $\tilde{R}_j = X_1 R_j X_1$  ( $j = 1, 2, 3$ ),  $\tilde{Q}_4 = X_2 Q_4 X_2$ ,  $\tilde{R}_4 = X_2 R_4 X_2$ ,  $\tilde{U}_{1k} = \tilde{M}_k = X_1 M_k X_1$ ,  $\tilde{U}_{2k} = \tilde{N}_k = X_1 N_k X_1$ ,  $\tilde{U}_{3k} = \tilde{S}_k = X_1 S_k X_1$ , and  $\tilde{W}_k = X_2 W_k X_2$  ( $k = 1, 2, 3, 4$ ) and then  $\tilde{\Theta}_i$  ( $i = 1, 2, 3$ ) and  $\tilde{\Theta}_4$  are obtained by pre- and post-multiplying both sides of  $\Theta_i$  ( $i = 1, 2, 3$ ) and  $\Theta_4$  with  $\text{diag}\{X_1, X_1, X_1, X_1\}$  and  $\text{diag}\{X_2, X_2, X_2, X_2\}$ , respectively.

Moreover, define  $Y_1 = K_1 X_1$ ,  $Y_2 = K_2 X_2$ . Pre- and post-multiply both sides of (44) with  $\text{diag}\{\underbrace{X_1, X_1, \dots, X_1}_{13}, \underbrace{X_2, X_2, \dots, X_2}_5, X_1, X_1, I, I, X_1, X_1, X_1, X_2, X_2, X_2, X_2, \underbrace{I, I, \dots, I}_6\}$ , and then substitute  $-\bar{\beta}\epsilon_f X_1 + \bar{\beta}\epsilon_f^2 I$  into  $-\bar{\beta}X_1 I X_1$ .

As a result, the (20) can be derived from (44) to guarantee the system (14) mean-square asymptotically stable, and the desired state feedback gain both of primary controller in (23) and secondary controller in (24) can be obtained at the same time.

This completes the proof.

## REFERENCES

- [1] J. Alvarez-Ramirez, J. Alvarez, and A. Morales, "An adaptive cascade control for a class of chemical reactors," *Int. J. Adapt. Control Signal Process.*, vol. 16, no. 10, pp. 681–701, 2002.
- [2] Y. Li, C. Cai, K.-M. Lee, and F. Teng, "A novel cascade temperature control system for a high-speed heat-airflow wind tunnel," *IEEE/ASME Trans. Mechatronics*, vol. 18, no. 4, pp. 1310–1319, Aug. 2013.
- [3] W. Luo, C. G. Soares, and Z. Zou, "Neural-network- and L2-gain-based cascaded control of underwater robot thrust," *IEEE J. Ocean. Eng.*, vol. 39, no. 4, pp. 630–640, Oct. 2014.
- [4] C. Huang, Y. Bai, and X. Liu, " $H_\infty$  state feedback control for a class of networked cascade control systems with uncertain delay," *IEEE Trans. Ind. Informat.*, vol. 6, no. 1, pp. 62–72, Feb. 2010.
- [5] J. Zhang and C. Peng, "Guaranteed cost control of uncertain networked control systems with a hybrid communication scheme," *IEEE Trans. Syst., Man, Cybern., Syst.*, to be published, doi: [10.1109/TSMC.2018.2833203](https://doi.org/10.1109/TSMC.2018.2833203).
- [6] Y. Bai and C. Z. Huang, "Analysis and modeling of a class of networked cascade control systems," *Inf. Control*, vol. 36, no. 3, pp. 273–277, 2007.
- [7] Z. Du, D. Yue, and S. Hu, " $\mathcal{H}_\infty$  stabilization for singular networked cascade control systems with state delay and disturbance," *IEEE Trans. Ind. Informat.*, vol. 10, no. 2, pp. 882–894, May 2014.
- [8] S. Srimanta, R. Sakthivel, Y. Shi, and K. Mathiyalagan, "Dissipative sampled-data controller design for singular networked cascade control systems," *J. Frankl. Inst.*, vol. 353, no. 14, pp. 3386–3406, 2016.
- [9] S. Srimanta, R. Sakthivel, K. Mathiyalagan, and S. M. Anthoni, "Exponential passivity results for singular networked cascade control systems via sampled-data control," *J. Dyn. Syst. Meas. Control*, vol. 139, no. 3, 2016, Art. no. 031001, doi: [10.1115/1.4034781](https://doi.org/10.1115/1.4034781).
- [10] Z. Wu, Y. Wu, Z. Wu, and J. Lu, "Event-based synchronization of heterogeneous complex networks subject to transmission delays," *IEEE Trans. Syst., Man, Cybern., Syst.*, to be published, doi: [10.1109/TSMC.2017.2723760](https://doi.org/10.1109/TSMC.2017.2723760).
- [11] D. Zhang, S. K. Nguang, and L. Yu, "Distributed control of large-scale networked control systems with communication constraints and topology switching," *IEEE Trans. Syst., Man, Cybern., Syst.*, vol. 47, no. 7, pp. 1746–1757, Jul. 2017.
- [12] L. Wang, Z. Wang, Q. Han, and G. Wei, "Event-based variance-constrained  $\mathcal{H}_\infty$  filtering for stochastic parameter systems over sensor networks with successive missing measurements," *IEEE Trans. Cybern.*, vol. 48, no. 3, pp. 1007–1017, Mar. 2018.
- [13] X.-M. Zhang, Q.-L. Han, and B.-L. Zhang, "An overview and deep investigation on sampled-data-based event-triggered control and filtering for networked systems," *IEEE Trans. Ind. Informat.*, vol. 13, no. 1, pp. 4–16, Feb. 2017.
- [14] D. Yue, E. Tian, and Q.-L. Han, "A delay system method for designing event-triggered controllers of networked control systems," *IEEE Trans. Autom. Control*, vol. 58, no. 2, pp. 475–481, Feb. 2013.
- [15] X. Xie, Q. Zhou, Y. Dong, and H. Li, "Relaxed control design of discrete-time Takagi–Sugeno fuzzy systems: An event-triggered real-time scheduling approach," *IEEE Trans. Syst., Man, Cybern., Syst.*, to be published, doi: [10.1109/TSMC.2017.2737542](https://doi.org/10.1109/TSMC.2017.2737542).
- [16] Z. Wu, Y. Xu, Y. Pan, P. Shi, and Q. Wang, "Event-triggered pinning control for consensus of multiagent systems with quantized information," *IEEE Trans. Syst., Man, Cybern., Syst.*, vol. 48, no. 11, pp. 1929–1938, Nov. 2018.
- [17] Z.-G. Wu, Y. Xu, R. Lu, Y. Wu, and T. Huang, "Event-triggered control for consensus of multiagent systems with fixed/switching topologies," *IEEE Trans. Syst., Man, Cybern., Syst.*, vol. 48, no. 10, pp. 1736–1746, Oct. 2018, doi: [10.1109/TSMC.2017.2744671](https://doi.org/10.1109/TSMC.2017.2744671).
- [18] X.-M. Zhang and Q.-L. Han, "Event-based  $\mathcal{H}_\infty$  filtering for sampled-data systems," *Automatica*, vol. 51, pp. 55–69, Jan. 2015.
- [19] C. Peng, Y. Dong, and M.-R. Fei, "A higher energy-efficient sampling scheme for networked control systems over IEEE 802.15.4 wireless networks," *IEEE Trans. Ind. Informat.*, vol. 12, no. 5, pp. 1766–1774, Oct. 2016.
- [20] L. Zha, E. Tian, X. Xie, Z. Gu, and J. Cao, "Decentralized event-triggered  $\mathcal{H}_\infty$  control for neural networks subject to cyber-attacks," *Inf. Sci.*, vols. 457–458, pp. 141–155, Aug. 2018.
- [21] J. Liu, L. Zha, J. Cao, and S. Fei, "Hybrid-driven-based stabilization for networked control systems," *IET Control Theory Appl.*, vol. 10, no. 17, pp. 2279–2285, Nov. 2016.
- [22] J. Liu, L. Wei, X. Xie, E. Tian, and S. Fei, "Quantized stabilization for T-S fuzzy systems with hybrid-triggered mechanism and stochastic cyber attacks," *IEEE Trans. Fuzzy Syst.*, to be published, doi: [10.1109/TFUZZ.2018.2849702](https://doi.org/10.1109/TFUZZ.2018.2849702).
- [23] J. Liu, L. Wei, J. Cao, and S. Fei, "Hybrid-driven  $\mathcal{H}_\infty$  filter design for T-S fuzzy systems with quantization," *Nonlin. Anal. Hybrid Syst.*, vol. 31, pp. 135–152, Feb. 2019.
- [24] J. Liu, L. Zha, X. Xie, and E. Tian, "Resilient observer-based control for networked nonlinear T-S fuzzy systems with hybrid-triggered scheme," *Nonlin. Dyn.*, vol. 91, no. 3, pp. 2049–2061, 2018.
- [25] J. Liu, L. Wei, E. Tian, S. Fei, and J. Cao, " $\mathcal{H}_\infty$  filtering for networked systems with hybrid-triggered communication mechanism and stochastic cyber attacks," *J. Frankl. Inst.*, vol. 354, no. 18, pp. 8490–8512, 2017.
- [26] J. Liu, J. Xia, E. Tian, and S. Fei, "Hybrid-driven-based  $\mathcal{H}_\infty$  filter design for neural networks subject to deception attacks," *Appl. Math. Comput.*, vol. 320, pp. 158–174, Mar. 2018.
- [27] A. Seuret and F. Gouaisbaud, "Wirtinger-based integral inequality: Application to time-delay systems," *Automatica*, vol. 49, no. 9, pp. 2860–2866, 2013.
- [28] P. Park, J. W. Ko, and C. Jeong, "Reciprocally convex approach to stability of systems with time-varying delays," *Automatica*, vol. 47, no. 1, pp. 235–238, 2011.
- [29] H. Zhang, Z. Wang, and D. Liu, "A comprehensive review of stability analysis of continuous-time recurrent neural networks," *IEEE Trans. Neural Netw. Learn. Syst.*, vol. 25, no. 7, pp. 1229–1262, Jul. 2014.
- [30] H. Zhang, Z. Wang, and D. Liu, "Global asymptotic stability of recurrent neural networks with multiple time-varying delays," *IEEE Trans. Neural Netw.*, vol. 19, no. 5, pp. 855–873, May 2008.
- [31] M. Chen, "Constrained control allocation for overactuated aircraft using a neurodynamic model," *IEEE Trans. Syst., Man, Cybern., Syst.*, vol. 46, no. 12, pp. 1630–1641, Dec. 2016.
- [32] Y. Yang, J. Tan, and Y. Dong, "Prescribed performance tracking control of a class of uncertain pure-feedback nonlinear systems with input saturation," *IEEE Trans. Syst., Man, Cybern., Syst.*, to be published, doi: [10.1109/TSMC.2017.2784451](https://doi.org/10.1109/TSMC.2017.2784451).
- [33] Q. Wang, Z. Wu, P. Shi, and A. Xue, "Robust control for switched systems subject to input saturation and parametric uncertainties," *J. Frankl. Inst.*, vol. 354, no. 16, pp. 7266–7279, 2017.
- [34] L. Sun, Y. Wang, and G. Feng, "Control design for a class of affine nonlinear descriptor systems with actuator saturation," *IEEE Trans. Autom. Control*, vol. 60, no. 8, pp. 2195–2200, Aug. 2015.
- [35] C. Yang, L. Zhang, and J. Sun, "Anti-windup controller design for singularly perturbed systems subject to actuator saturation," *IET Control Theory Appl.*, vol. 10, no. 4, pp. 469–476, Feb. 2016.
- [36] H. Li, L. Bai, Q. Zhou, R. Lu, and L. Wang, "Adaptive fuzzy control of stochastic nonstrict-feedback nonlinear systems with input saturation," *IEEE Trans. Syst., Man, Cybern., Syst.*, vol. 47, no. 8, pp. 2185–2197, Aug. 2017.
- [37] B. Wang, J. Wang, B. Zhang, and X. Li, "Global cooperative control framework for multiagent systems subject to actuator saturation with industrial applications," *IEEE Trans. Syst., Man, Cybern., Syst.*, vol. 47, no. 7, pp. 1270–1283, Jul. 2017.
- [38] D. Liu and G.-H. Yang, "Event-triggered control for linear systems with actuator saturation and disturbances," *IET Control Theory Appl.*, vol. 11, no. 9, pp. 1351–1359, Feb. 2017.
- [39] A. Wei, Y. Song, and C. Wen, "Adaptive cyber-physical system attack detection and reconstruction with application to power systems," *IET Contr. Theory Appl.*, vol. 10, no. 12, pp. 1458–1468, Aug. 2016.
- [40] L. An and G.-H. Yang, "Improved adaptive resilient control against sensor and actuator attacks," *Inf. Sci.*, vol. 423, pp. 145–156, Jan. 2018.

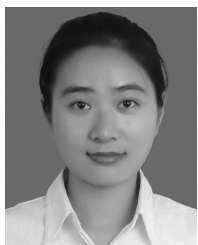
- [41] D. Ding, G. Wei, S. Zhang, Y. Liu, and F. E. Alsaadi, "On scheduling of deception attacks for discrete-time networked systems equipped with attack detectors," *Neurocomputing*, vol. 219, pp. 99–106, Jan. 2016.
- [42] D. Zhang, L. Liu, and G. Feng, "Consensus of heterogeneous linear multi-agent systems subject to aperiodic sampled-data and DoS attack," *IEEE Trans. Cybern.*, to be published, doi: [10.1109/TCYB.2018.2806387](https://doi.org/10.1109/TCYB.2018.2806387).
- [43] E. Mousavinejad, F. Yang, Q.-L. Han, and L. Vlacic, "A novel cyber attack detection method in networked control systems," *IEEE Trans. Cybern.*, vol. 48, no. 11, pp. 3254–3264, Nov. 2018.
- [44] D. Ding, Z. Wang, Q.-L. Han, and G. Wei, "Security control for discrete-time stochastic nonlinear systems subject to deception attacks," *IEEE Trans. Syst., Man, Cybern., Syst.*, vol. 48, no. 5, pp. 779–789, May 2018.
- [45] D. Ding, Z. Wang, D. W. C. Ho, and G. Wei, "Observer-based event-triggering consensus control for multiagent systems with lossy sensors and cyber-attacks," *IEEE Trans. Cybern.*, vol. 47, no. 8, pp. 1936–1947, Aug. 2017.
- [46] J. Liu, E. Tian, X. Xie, and L. Hong, "Distributed event-triggered control for networked control systems with stochastic cyber-attacks," *J. Frankl. Inst.*, Mar. 2018, doi: [10.1016/j.jfranklin.2018.01.048](https://doi.org/10.1016/j.jfranklin.2018.01.048).
- [47] D. Ding, Z. Wang, D. W. C. Ho, and G. Wei, "Distributed recursive filtering for stochastic systems under uniform quantizations and deception attacks through sensor networks," *Automatica*, vol. 78, pp. 231–240, Apr. 2017.
- [48] J. Liu, Y. Gu, J. Cao, and S. Fei, "Distributed event-triggered  $\mathcal{H}_\infty$  filtering over sensor networks with sensor saturations and cyber-attacks," *ISA Trans.*, Aug. 2018, doi: [10.1016/j.isatra.2018.07.018](https://doi.org/10.1016/j.isatra.2018.07.018).



**Jinliang Liu** received the Ph.D. degree from the School of Information Science and Technology, Donghua University, Shanghai, China.

He was a Post-Doctoral Research Associate with the School of Automation, Southeast University, Nanjing, China, from 2013 to 2016. From 2016 to 2017, he was a Visiting Researcher/Scholar with the Department of Mechanical Engineering, University of Hong Kong, Hong Kong. From 2017 to 2018, he was a Visiting Scholar with the Department of Electrical Engineering, Yeungnam University,

Gyeongsan, South Korea. He is currently an Associate Professor with the Nanjing University of Finance and Economics, Nanjing, China. His current research interests include networked control systems, complex dynamical networks, T-S fuzzy systems, and time delay systems.



**Yuanyuan Gu** was born in Jiangsu Province, China, in 1994. She received the B.S. degree from Xuzhou Medical University, Xuzhou, China, in 2016. She is currently pursuing the M.S. degree from the College of Information Engineering, Nanjing University of Finance and Economics, Nanjing, China.

Her current research interests include networked control systems, power systems, and time delay systems.



**Xiangpeng Xie** received the B.S. and Ph.D. degrees in engineering from Northeastern University, Shenyang, China, in 2004 and 2010, respectively.

From 2012 to 2014, he was a Post-Doctoral Fellow with the Department of Control Science and Engineering, Huazhong University of Science and Technology, Wuhan, China. He is currently an Associate Professor with the Research Institute of Advanced Technology, Nanjing University of Posts and Telecommunications, Nanjing, China. His current research interests include fuzzy modeling and

control synthesis, state estimations, optimization in process industries, and intelligent optimization algorithms.



**Dong Yue** received the Ph.D. degree from the South China University of Technology, Guangzhou, China, in 1995.

He is currently a Professor and the Dean with the Research Institute of Advanced Technology, Nanjing University of Posts and Telecommunications, Nanjing, China, and also a Changjiang Professor with the Department of Control Science and Engineering, Huazhong University of Science and Technology, Wuhan, China. He has published over 100 papers in international journals, domestic

journals, and international conferences. His current research interests include analysis and synthesis of networked control systems, multiagent systems, optimal control of power systems, and Internet of Things.

Dr. Yue is currently an Associate Editor of the IEEE Control Systems Society Conference Editorial Board and the *International Journal of Systems Science*.



**Ju H. Park** received the Ph.D. degree in electronics and electrical engineering from the Pohang University of Science and Technology (POSTECH), Pohang, South Korea, in 1997.

He was a Research Associate with the Engineering Research Center-Automation Research Center with POSTECH from 1997 to 2000. In 2000, he joined Yeungnam University, Gyeongsan, South Korea, where he is currently the Chuma Chair Professor. From 2006 to 2007, he was a Visiting Professor with the Department of Mechanical

Engineering, Georgia Institute of Technology, Atlanta, GA, USA. His current research interests include robust control and filtering, neural networks, complex networks, multiagent systems, and chaotic systems. He has authored a number of papers in the above areas.

Prof. Park was a recipient of the Highly Cited Researcher Award by Clarivate Analytics (formerly, Thomson Reuters) since 2015. He serves as an Editor for *International Journal of Control, Automation, and Systems*. He is also a Subject Editor/Associate Editor/Editorial Board Member for several international journals, including *IET Control Theory and Applications*, *Applied Mathematics and Computation*, *Journal of the Franklin Institute*, *Nonlinear Dynamics*, *Journal of Applied Mathematics and Computing*, *Cogent Engineering*, and IEEE TRANSACTIONS ON FUZZY SYSTEMS. He is a FELLOW of the Korean Academy of Science and Technology.